Computational Studies of Silver Clusters Adsorbed on AgBr Cubic Surfaces

Roger C. Baetzold

Imaging Research and Advanced Development, Eastman Kodak Company, Rochester, New York

Silver clusters adsorbed to different sites on cubic AgBr surfaces have been treated by classical and quantum mechanical methods. The properties computed include structure, bond energies, and ionization energies. The optimized geometry of the adsorbed silver cluster tends to be planar up to and including four atoms in size. Distinct odd–even oscillations in the ionization potential and electron affinity, similar to those known in the gas phase, are found for the adsorbed silver clusters. The site of adsorption exerts a strong effect on the calculated energy levels consistent with Coulombic reasoning based upon formal partial site charges. Structural relaxation of the clusters plays an important role in their electron accepting properties. The Ag_2 and Ag_4 clusters have a large ionization potential, which correlates with high stability. The Ag_3 cluster is less stable, due to midgap levels capable of accepting electrons or holes. Overall, the calculations are consistent with the nucleation and growth model of latent image formation.

Journal of Imaging Science and Technology 43: 30–37 (1999)

Introduction

Microscopic understanding of the initial steps in the photolysis of silver halide has come from a variety of deductions derived from experiment. These are well summarized[1–3] and have been assembled into detailed mechanisms such as the nucleation and growth model. This mechanism consists of alternate stepwise processes involving electrons and interstitial silver ions leading to the growth of a silver cluster. Special sites on the surface are believed to impart a formal partial charge to the growing cluster, which provides a driving force for collection of silver atoms at that site. While the photophysics of silver halide has been well described[4] the energy levels of the adsorbed silver clusters, as well as many of their electronic properties, are not well known. Theoretical modeling can play a role in elucidating these properties.

We have previously attempted[5,6] to construct a model for latent image growth based upon theoretical considerations. Such a model is based upon the total energy of various possible intermediate reaction species that may be present during photolysis. Only qualitative models could be constructed at that time due to limitations of computer capability and in the ability to treat the important interactions present in this system. It is known that both ionic and covalent bonding interactions in silver halide are important, and so a method treating these, such as CNDO (complete neglect of differential overlap), was considered at least a baseline requirement for the problem. One of the key findings of that work[6] was the result that the site of adsorption for the silver clusters on the silver halide played a strong role in determining its electronic properties. Several other calculations[7–12] using atomistic or quantum mechanical methods have appeared, and some support this conclusion.

The first calculations were approximate because of limitations of the CNDO technique, small model size, and arbitrary placement of cluster atoms at lattice sites on the model. Despite these limitations the calculations provided an explanation for why silver clusters behaved differently depending on their location on the grain surface. Experiments by Spencer, Brady, and Hamilton[13] showed two types of silver centers were present on grains, termed R and P centers. It was proposed[14] that the chemically produced R centers trap holes and disappear while the photolytically produced P centers trap electrons and grow during light illumination. During the same period, Tani[15] was investigating similar centers and attributing differences between the hole and electron trapping centers to the sites where they form on the crystal. The CNDO calculations[6] showed that the highest occupied energy level of Ag_2 was above the valence band edge of AgBr at neutral surface sites, but below the valence band edge at positive sites such as the positive kink site. Thus, on energetic grounds a photohole could only be trapped at Ag_2 residing at a surface site of neutral charge but not at the positive kink. This led to the assignment that these silver particles at neutral sites were the R centers and corresponding particles at the positive kink site were the P centers. More recent[16–18] detailed experimental studies have supported this assignment.

A comprehensive dynamic computer model of silver cluster formation within AgBr microcrystals was constructed.[19] This was based upon detailed understanding or assumptions concerning the individual steps involved in each stage of the process. Specific knowledge of some of these stages is often incomplete and a comprehensive model of the energetics of these steps may help to elaborate various details. One example where this may apply involves the proposal of a strong

Original manuscript received January 28, 1998

coupling between the electron and silver halide trapping site.[2,20,21] This proposal has been advanced based upon analysis of photographic data and the factors involved in nonradiative transitions in other semiconductors and insulators.[21] We will investigate this possibility directly by computing the total energy changes that can occur by geometric relaxation at a silver cluster following trapping of an electron.

We turn to the application of modern computational methodologies to the latent image formation problem. The approach will be to derive the energetics of steps in the process and deduce a likely mechanism. Of course, these considerations only indicate whether a pathway is energetically feasible, whereas kinetic factors are involved in the actual growth mechanism. These kinetic factors could be influenced by Coulombic interactions as mediated by the high dielectric constant of silver halide. We will apply several advances in computational methodology to this problem. An *ab initio* quantum mechanical method that can be used to optimize the adsorbed silver cluster geometry, while treating the long range Coulomb and lattice polarization effects in silver halide, will be employed. We choose sites on the cubic nonpolar surface for examination because these can be well defined. The important characteristic of these sites is their charge, which may also apply to other surfaces where different local sites may be present.

The plan of this work is to treat each aspect of latent image formation with a method most appropriate to that particular phase of the problem. For example, ionic steps involving the binding of a silver ion or vacancy are best treated by the atomistic classical method, where the necessary interatomic potentials are found in quantum mechanical calculations and where the long-range lattice polarization is directly calculated. But electron or hole trapping at a silver cluster involves charge redistribution and requires a quantum mechanical treatment to describe this phase of the problem. In the Method section we discuss the computational methodologies applied to this problem. These include classical atomistic and quantum mechanical methods. In the Results section we discuss the calculated electronic properties of adsorbed silver clusters. These include the energy changes involving Ag^+ ions and the growth of clusters. We also determine the electron and hole trapping properties of silver clusters adsorbed at different surface sites. In the Discussion section we examine the effects of site geometry, cluster size, and charge on electronic properties and compare to available experiments.

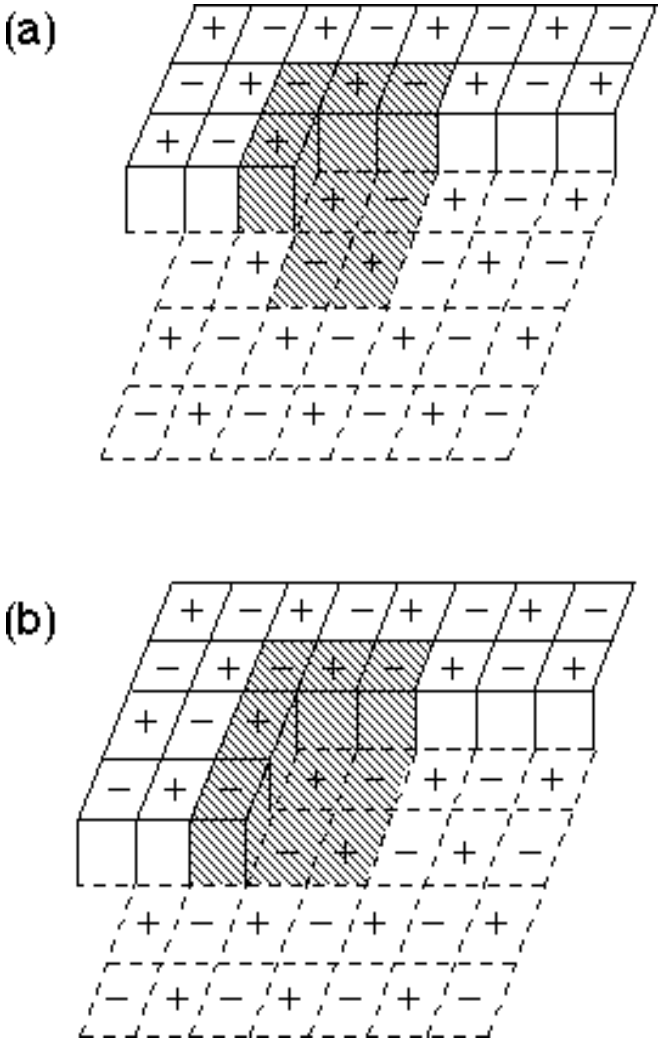

Figure 1. Sketches of the (a) positive kink (+K) model and (b) double kink (+DK) models considered in this work. The complementary sites obtained by interchanging positive and negative ions are the negative kink (–K) and double kink (–DK). The shaded ions represent the explicit quantum mechanical ions considered in the *ab initio* calculations.

Method

Classical Atomistic. The classical atomistic method relies upon the use of interatomic potentials to treat all the interaction of adsorbed species with lattice silver halide ions. The interatomic potentials[22,23] include components due to Coulombic interactions, short-range overlap of electron clouds, and polarization effects. All of these effects are treated self-consistently. The potentials reproduce the bulk rock salt structure of AgBr giving an equilibrium Ag–Br distance of 2.864 Å and have been used to treat a variety of properties including defect formation and its temperature dependence.[24] Quantum mechanical calculations treating electron correlation are necessary to devise the potentials for the silver cluster and its interaction with the silver halide surface. The lattice relaxation caused by defects such as interstitial silver ions or vacancies are treated within the scope of the Mott–Littleton approximation[25] in order to compute the energy. These approaches have been extended to surfaces[26] and can be used to treat silver clusters adsorbed to various sites on a surface. We have previously[27] shown how this method can be applied to this problem and the detailed nature of the interatomic potentials that are required.

We are interested in treating Ag clusters adsorbed to kinks, steps, or terraces on cubic AgBr surfaces. The single and double kink models are sketched in Fig. 1. Our notation describes positive kinks (+K), negative kinks (-K), double kinks with negative inner ions (–DK) or positive inner ions (+DK), and (100) surfaces (flat). Models for these sites have been constructed[27] within the scope of the classical atomistic model where the reader can turn for details. The positions of the atoms in a silver cluster next to each surface defect are calculated by full geometry optimization. This procedure takes into account the short-range interatomic functions described earlier as well as Coulomb interactions such as those arising when the cluster is charged. The total energy resulting from the optimization can be compared to the total energy of the separated cluster and surface defect model in order to compute an adsorption energy. The adsorption energy includes effects due to the short-range

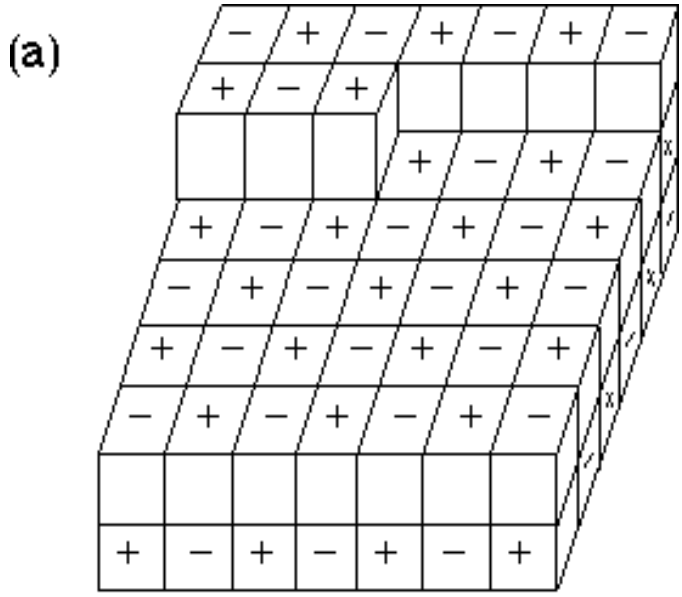

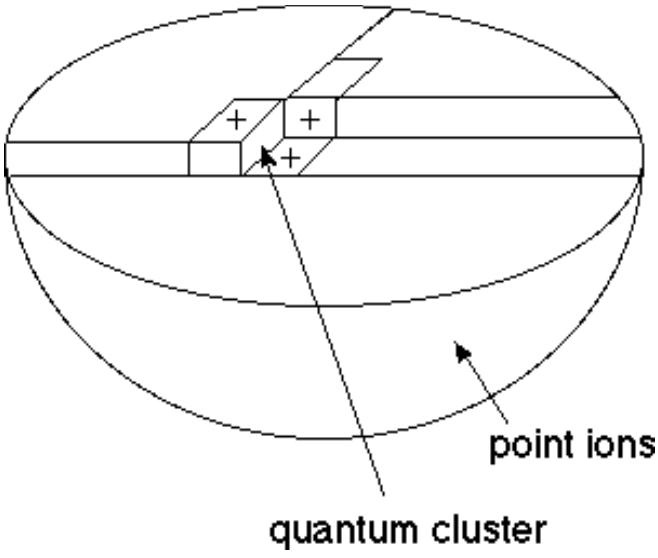

Figure 3. Sketch of the hemispherical point ion array used in the *ab initio* calculations. The sketch shows a +K model.

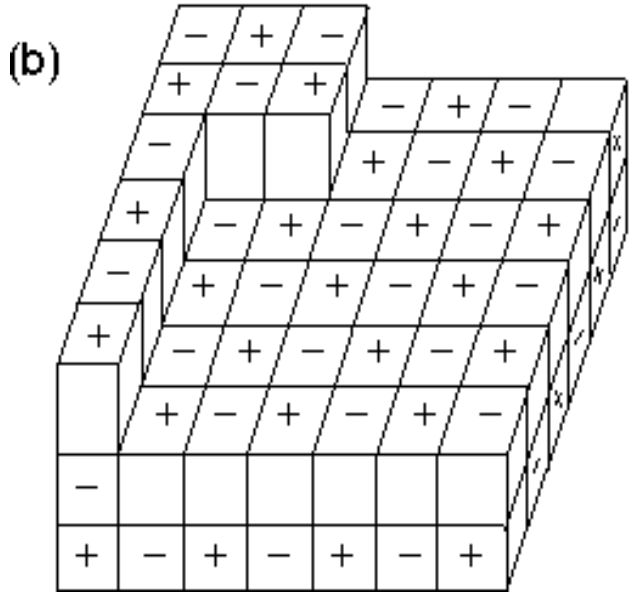

Figure 2. The $(AgBr)_{47}$ units used for the (+K) in (a) and (–DK) in (b) are shown. The complementary (–K) and (+DK) units are obtained by interchanging positive and negative ions.

interactions as well as those due to crystal polarization that become more important for charged clusters.

Semiempirical Quantum Mechanical. We have previously[6] employed a CNDO method to treat silver clusters adsorbed to AgBr models. In the present work we extend the model size. In earlier work the silver clusters were placed at virtual lattice sites near the surface site. In the present work these atoms are placed at positions determined in *ab initio* quantum mechanical calculations. However, with the improvements in model size and cluster placement this calculation is regarded as approximate and chiefly used to discern trends. It is a purely cluster method, as we use it here, with no background field due to omitted lattice ions. Thus, the trends that emerge from this calculation are independent of any assumptions regarding the silver halide crystal ionicity.

The CNDO cluster models constructed for the different surface sites are rectangular in overall shape and are shown in Fig. 2. We considered $(AgBr)_{47}$ units for the single and double kink sites and $(AgBr)_{42}$ for the flat site where only the two bottom layers in Fig. 2 are considered.

***Ab Initio* Calculations.** We employ the local density method based upon exchange and correlation components and termed the BYLP functional.[28] Silver ions and atoms are treated with a model potential.[29] The 4p, 4d, and 5s valence orbitals lie outside the pseudopotential and are treated with the basis orbitals. The number of electrons added to the system is determined by the charge of the silver cluster, and thus the same core potential is employed for both atom and ion. The basis sets for Ag are double zeta with polarization, and for Br are full basis sets at the double zeta level. The sources of these parameters have been described before.[30] The computer code CADPAC[31] is used for these calculations. We create a surface model using roughly 1200 point ions as sketched in Fig. 3. The model is roughly hemispheric in shape having unit charges at the appropriate Ag^+ and Br^- sites of AgBr with overall zero charge. A surface partial layer of charges is constructed to form a particular defect such as the positive kink shown in Fig. 1. Several of the point charges are replaced by quantum mechanical ions near the kink site. The appropriate ions are shaded as indicated in Fig. 1. Thus, we consider Ag_4Br_4 for (+K) and (-K), Ag_5Br_4 for (–DK), and Ag_5Br_4 for (100) flat surfaces. Given these defect sites, the silver cluster containing from one to four atoms is placed near this site, and its geometry is fully optimized to yield an equilibrium structure and energy. Following this procedure a second calculation is undertaken to compute the AgBr lattice relaxation energy. This second calculation employs the atomistic method as applied to the appropriate surface defect model plus silver cluster. The position and charge of ions determined quantum mechanically are fixed and the rest of the crystal ions allowed to relax. The sum of the quantum mechanical and relaxation energies is used

to compute the ionization potential (IP) and electron affinity (EA). We calculated the conduction band edge at 3.6 eV and valence band edge at 6.2 eV using cluster models within the embedded cluster model described before.[32] Details of the method are available,[32] as well as the full set of interatomic potentials derived from the method.

Results

Ionic Reactions. We first consider ionic reactions leading to point defect generation from the surface. These can be written for kink sites

$$+\mathrm{K} \rightleftarrows -\mathrm{K} + \mathrm{Ag}_i^+, \quad (1)$$

$$-\mathrm{K} + \mathrm{Ag}_L^+ \rightleftarrows +\mathrm{K} + \mathrm{V}, \quad (2)$$

where Ag_i^+ is the interstitial silver ion, Ag_L^+ is the corresponding lattice ion, V is the silver ion vacancy, and we employ the +K, –K kink notation described before.

The energy change for point defect formation at the surface may be computed with the classical atomistic methods. We have previously[27] shown how this may be done. In this work we take as reference a bulk interstitial or vacancy energy corrected for the surface rumpling at a (100) surface.[33] This yields 0.35 and 0.88 eV for the formation of interstitial and vacancy, respectively, from kinks on the (100) AgBr surface. These values represent enthalpy terms at 0 K for the forward reactions in Eqs. 1 and 2, and indicate that it is easier to form interstitials than vacancies from surface sites.

We have extended the ionic defect formation calculations to AgBr surface sites containing silver atom clusters. The classical atomistic method is employed. A silver cluster is placed on a surface site and along with all of the crystal ions allowed to relax to achieve an equilibrium configuration. Thus, the orientation of the cluster relative to the defect site and the cluster shape itself is optimized. The silver clusters interact strongly with the surface. The distance to ions at the positive kink is 2.56 Å for Ag, 2.41 Å for Ag^-, and 4.54 Å for Ag^+. These distances represent energy minima for the adsorbed clusters. We find that the cluster tends to remain near planar in shape and orients in particular directions near the defect site. Thus, the near triangular and rectangular shapes for Ag_3 and Ag_4, respectively, are found. It is interesting that Ag_2 prefers to orient with its bond at roughly 45° to the ledge directions near a single or double kink. We find this orientation persists in the larger clusters where additional atoms are added to this center. These geometries are very similar to those found in our *ab initio* calculations, which we shall display and discuss in more detail later. Using the optimized structures we compute adsorption energies at the different sites in Table I. It is apparent from the magnitudes of these quantities that a significant interaction is occurring between the silver atoms and AgBr substrate. Note that the adsorption energy contains components arising from short-range interactions and polarization of the AgBr crystal. This is why cationic clusters have larger adsorption energies than their neutral counterparts. The electrostatic terms between the surface defect and cluster become manifest when adsorption energies are compared at different sites. The cationic clusters are adsorbed more strongly at the negative kink site and usually follow the order (–K) > (–DK) > (+DK) > (+K), that is expected based upon the site charge.

We first consider the stability of the Ag^0 atom on various AgBr surface sites. We consider the reaction

$$\mathrm{Ag}^0 + -\mathrm{K} \rightleftarrows +\mathrm{K} + \mathrm{e}_{\mathrm{CB}}, \quad (3)$$

where the Ag atom is adsorbed at different possible sites and can decay by releasing a silver ion that diffuses to a negative kink (–K) converting it to a positive kink (+K) followed by release of an electron to the conduction band (e_{CB}). Formation of the silver atom occurs by the reverse reaction. Using the adsorption energy values in Table I and a value of –4.57 eV for the conduction band edge,[33] we calculate the energy change for Reaction 3 where the silver atom is placed at a variety of different surface sites in Table II. On all sites except the flat (100) surface this reaction is endothermic. This indicates that the Ag atom is stable, but because of the small energy change this reaction is consistent with a temporary lifetime of the Ag atom. This result is in line with photographic measurements[34,35] indicating a finite lifetime of the Ag atom.

Silver clusters can potentially exchange silver ions with point defects and surface defect sites on AgBr. We have examined the energy changes for several of these possible reactions.

$$(\mathrm{site} \cdot \mathrm{Ag}_{n+1})^+ \rightleftarrows (\mathrm{site} \cdot \mathrm{Ag}_n) + \mathrm{Ag}_i^+, \quad (4)$$

$$(\mathrm{site} \cdot \mathrm{Ag}_{n+1})^+ + \mathrm{V} \rightleftarrows (\mathrm{site} \cdot \mathrm{Ag}_n), \quad (5)$$

$$(\mathrm{site} \cdot \mathrm{Ag}_{n+1})^+ + -\mathrm{K} \rightleftarrows (\mathrm{site} \cdot \mathrm{Ag}_n) + +\mathrm{K}. \quad (6)$$

We consider a specific site for each reaction and denote Ag_i^+ as the interstitial silver ion, V as the vacancy, –K as the negative kink, and +K as the positive kink. We have used the normal calculated bulk interstitial energy (–4.31 eV) and vacancy energy (5.44 eV) as well as the adsorption energies (Table I) to arrive at the values in Table III. It has also been necessary to correct the bulk reference values for rumpling effects[3,4] at the (100) surface, which slightly shifts the bulk reference values.

The equilibrium of silver ions with surface silver clusters can be examined with the data in Table III. At the positive kink only the Ag_3^+ cluster is stable with respect to loss of a silver ion to an interstitial position. At the

TABLE I. Adsorption Energies (eV) of Ag Clusters on AgBr Surface Sites Calculated by Classical Atomistic Method

Cluster	+K	–K	+DK	–DK	Flat
Ag^0	2.01	2.23	1.89	2.21	0.92
Ag^+	3.10	4.45	2.62	3.77	3.34
Ag_2	3.89	5.47	3.47	3.17	1.49
Ag_2^+	4.54	6.03	5.01	5.29	3.51
Ag_3	6.34	6.35	6.22	6.09	2.02
Ag_3^+	6.98	8.21	6.93	7.58	3.61
Ag_4	7.39	6.89	6.93	7.42	4.12
Ag_4^+	7.90	8.74	7.10	7.78	5.30

TABLE II. Energy Change (eV) for Ag Atom Decay at Adsorbed AgBr Sites Using Atomistic Calculations

$Ag^0 + -K - \rightleftarrows +K + e_{CB}$	
Site	E
+K	0.62
–K	0.84
+DK	0.50
–DK	0.82
flat	–0.43

TABLE III. Energy Change* for Forward Reactions of Silver Ion at Adsorbed Silver Clusters on AgBr Calculated using Atomistic Calculations

(A) Site $Ag_{n+1}^+ \rightleftarrows$ site $Ag_n + Ag_i^+$

n	+K	–K	+DK	–DK	Flat
1	–0.05	1.22	0.54	0.50	0.01
2	0.35	0.00	0.72	1.67	–0.62
3	–0.13	0.70	0.91	0.00	1.59

(B) site $Ag_{n+1}^+ + V \rightleftarrows$ site Ag_n

1	–1.28	–0.01	–0.69	–0.73	–1.22
2	–0.88	–1.23	–0.51	0.44	–1.95
3	–1.36	–0.53	–2.14	–1.23	–0.36

(C) site $Ag_{n+1}^+ + -K \rightleftarrows +K +$ site Ag_n

1	–0.40	0.87	0.19	0.15	–0.34
2	0.00	–0.35	0.37	1.32	–0.97
3	–0.48	0.35	–1.26	–0.35	1.24

*Negative values indicate exothermic forward reaction.

TABLE IV. Energy Change (eV) for Ag Atom Aggregation

$n\ Ag^0 \rightarrow Ag_n^0$

n	+K	–K	+DK	–DK	Flat
2	–1.37	–2.51	–1.19	–0.25	–1.15
3	–2.47	–1.82	–2.71	–1.62	–1.42
4	–2.67	–1.29	–2.69	–1.90	–3.76

other sites the Ag_2^+, Ag_3^+, and Ag_4^+ are stable with respect to this reaction. However, in the presence of cation vacancies the energetics favor loss of Ag^+ from all of the cationic silver clusters involved. Finally, when we consider loss of the silver ion from the cationic silver cluster to a surface negative kink, most of the Ag_n^+ clusters are unstable. This reaction may be very important at the surface where negative kinks are in excess and would tend to favor stability of the neutral Ag_n cluster particularly when located at the positive kink site, which is important for latent image formation.

There is a strong driving force for aggregation of silver atoms to larger clusters. The reaction

$$n\ Ag^0 \rightarrow Ag_n^0 \qquad (7)$$

can be considered on the AgBr surface. Using the adsorption energy values in Table I and the calculated Ag_n bond energies (1.50 eV, $n = 2$; 2.16 eV, $n = 3$; 3.32 eV, $n = 4$) we compute the reaction energies in Table IV. The reaction is exothermic at each site, which is consistent with the growth of silver clusters. Thus, the pathway for growth at the positive kink involving electron capture followed by interstitial silver ion capture leads to clusters of overall greater stability as cluster size increases.

Semiempirical Calculations. A semiempirical CNDO procedure was used to study the trends in energy levels of silver clusters adsorbed to AgBr. We could easily treat about a hundred ions with this method. This is a simplified approach because it involves no explicit lattice polarization, and we base the AgBr conduction band edge on the electron affinity calculated for a $7 \times 6 \times 2$ rectangular array or AgBr ions. We calculate 3.5 eV for this value based upon the parameters in Table V. These parameters also give reasonable values for the IP and EA of gas phase silver clusters, which are shown in Table V. The gas phase clusters were considered at equilibrium bond lengths determined in *ab initio* calculations. We adsorb these clusters to the AgBr surface models at positions determined by *ab initio* calculations.

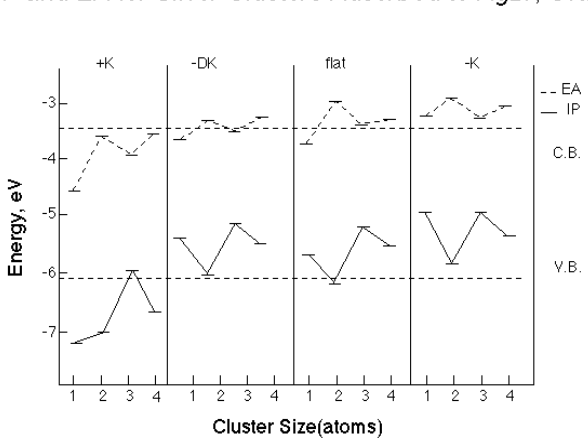

Figure 4. Values of ionization potential and electron affinity (eV) calculated by CNDO for silver clusters adsorbed at different surface sites. The calculated conduction band edge and corresponding valence band edge are shown.

TABLE V. Parameters and Results of CNDO Calculations

(A) Parameters

	Orbital	Exponent	β (eV)	-1/2 (I+A)(eV)
Ag	5s	1.35	–2	4.26
	5p	1.35	–2	2.39
Br	4s	1.86	–5	24.35
	4p	1.86	–5	5.61

(B) Computed IP and EA of Gas Phase Ag Clusters

	IP(eV)		EA(eV)	
	Calc	exp.*	Calc	exp.
Ag	7.29	7.57	1.23	1.30
Ag_2	7.88	7.56	1.14	1.02
Ag_3	6.54	6.20	1.88	2.43
Ag_4	6.67	6.65	2.04	1.65

*See Ref. 32 for the source of these values.

We compute the IP and EA values of the various Ag clusters adsorbed to AgBr by the difference in total energy of the appropriate charge states. These are plotted in Fig. 4 relative to the crystal reference levels where we examine trends in the calculation. The Ag clusters adsorbed to the positive kink give EA values slightly greater than the AgBr crystal EA value. Thus, all of these neutral clusters could trap an electron from the conduction band. This result contrasts with the behavior of Ag clusters at the other surface sites. In those cases, most of the neutral Ag clusters cannot trap a photoelectron because their EA value is less than the crystal EA. The IP values of most clusters lie in the band gap region making these suitable traps for a photohole. The Ag_n cluster at the positive kink site (except for Ag_3) present an exception to this behavior. These clusters would not be expected to act as a trap for photoholes. It is interesting that in these CNDO calculations, the IP and EA values are larger when the site has a partial positive charge and tend to be smaller as the site charge becomes negative. This result is in accord with the considerations of Seitz[36] and in accord with assumptions inherent in the nucleation and growth model.[2]

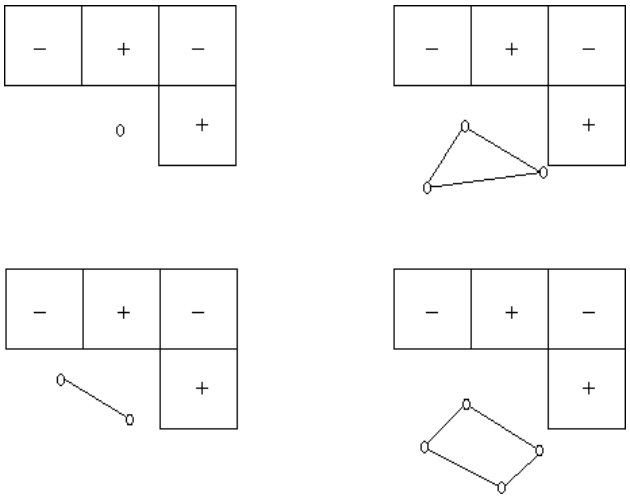

Figure 5. Sketch of the calculated equilibrium positions for neutral silver clusters near +K models using *ab initio* method described in the text. The crystal ions are enclosed in boxes and the silver atoms denoted by a circle.

TABLE VI. Coordinates Calculated for Silver Clusters near the Positive Kink. Positions are measured relative to the virtual site at (000) with positive values away from the crystal in au units

Cluster	Charge	*x*	*y*	*z*
Ag	0	0.12	0.20	0.30
Ag	–1	–0.17	0.35	0.39
Ag_2	0	–0.47	1.70	0.79
		4.26	0.00	0.32
Ag_2	–1	–0.11	0.54	0.52
		4.53	2.55	2.11
Ag_3	0	3.45	–0.33	1.94
		–0.89	2.68	2.10
		4.86	4.69	2.10
Ag_3	–1	3.76	–0.25	1.71
		–1.16	2.00	1.56
		5.18	4.64	2.33
Ag_4	0	1.60	8.65	2.10
		2.28	–0.54	1.96
		–1.13	2.66	2.12
		5.20	4.92	2.09
Ag_4	–1	1.52	8.53	2.19
		3.15	–0.45	1.83
		–1.27	2.62	1.70
		4.76	4.60	2.16

***Ab Initio* Calculations.** The *ab initio* calculations were used to compute the equilibrium geometry of the adsorbed silver clusters and have been refined since earlier work.[32] We find that the near planar geometry is favored at the sites considered here. The actual optimized coordinates for Ag_n clusters near kink sites are plotted in Fig. 5 and presented in Table VI. As indicated earlier for the atomistic calculations, the Ag_2 cluster becomes oriented with its bond midpoint near the virtual site for addition of the next ion near both the positive and double kink. This structure persists in Ag_3 and Ag_4 with additional atoms being added to form triangular and trapezoidal structures. These are the favored structures for the neutral clusters, and some relaxation from these structures occurs when an extra electron is added.

The distance from adsorbed silver cluster atoms to the surface ions is calculated to be comparable to interatomic bonding distances in the crystal. For example, the distance from a silver atom adsorbed at the positive kink to the nearest surface silver ions is calculated to be 2.97 Å, 2.93 Å, and 3.03 Å. The atom position is very

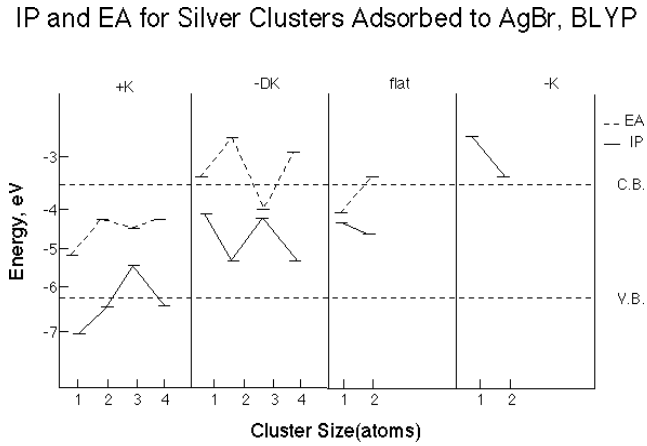

Figure 6. Values of ionization potential and electron affinity calculated for silver clusters of different size on various AgBr surface sites using the *ab initio* method with the BLYP functional.

TABLE VII. Calculated Ionization Potentials and Electron Affinity of Silver Clusters on AgBr Surface Sites—BLYP Method

Cluster	Site	IP(eV)	EA(eV)
Ag	+K	7.08	5.18
Ag_2	+K	6.41	4.28
Ag_3	+K	5.69	4.56
Ag_4	+K	6.49	4.20
Ag	–DK	4.01	3.37
Ag_2	–DK	5.35	2.56
Ag_3	–DK	3.95	4.11
Ag_4	–DK	5.23	3.05
Ag	flat	4.36	4.25
Ag_2	flat	4.61	3.49
Ag	–K	3.72	–0.09
Ag_2	–K	2.45	–4.81
AgAu	+K	6.94	4.81
Au	+K	8.56	5.72
Au_2	+K	8.21	6.12
Au_3	+K	6.10	6.09
Au_4	+K	6.20	4.80

close to the virtual lattice site for the kink. The silver anion has distances of 3.05 Å, 2.79 Å, and 3.08 Å to the surface silver ions. Of course, the larger silver clusters do not occupy near virtual sites as can be seen in Fig. 5 where the neutral cluster atoms are sketched near the positive kink. The distances of the Ag_2 cluster atoms from the nearest surface ions are 3.79 Å and 2.80 Å for one atom and 3.64 Å and 3.48 Å for the other atom. The situation becomes very complex as the number of cluster atoms increases, and so we report the atom positions for various clusters in Table VI. The distances reported for the positive kink site are comparable to those found at the double kink sites and negative kink. On the flat (100) surface the distances become larger in the range of 3.5 to 3.6 Å for adsorbed Ag or Ag_2. This result indicates a weaker interaction of the flat surface and is consistent with the smaller adsorption energies reported in the atomistic calculations for the flat surface in Table I.

We consider the electron affinity and ionization potential of these neutral clusters in Fig. 6 and Table VII. These values are calculated using the equilibrium structures for each charge state. There is a distinct shift in energy for both IP and EA at the different sites. The values are largest at the positive kink site where all EA values exceed the conduction band edge. Thus, each of these clusters are energetically capable of trapping a photoelectron. There is an oscillation in EA values consistent with a greater EA for the open shell cases. These

traps are of a depth such that the electron will have a finite lifetime in the anion state. The reversible release of this electron is expected unless an interstitial silver ion can neutralize this center. The IP also shows distinct oscillations at the positive kink. The Ag_2 center cannot trap a photohole because its IP is greater than the valence band edge. We observe oscillations in the IP and EA at the other sites where many of the centers cannot trap a photoelectron and are thus not possible latent image centers. These trends agree well with the trends calculated by the CNDO method.

We have tested whether trapping of an electron causes structural relaxation at the silver cluster. This was studied at the positive kink by first allowing the neutral cluster to relax fully to its equilibrium atom positions. An electron is added to the adsorbed cluster and further relaxation to the new equilibrium positions permitted. The change in energy upon this second relaxation is 0.14, 0.35, 0.20, and 0.10 eV for Ag, Ag_2, Ag_3, and Ag_4, respectively. This effect is a manifestation of strong coupling of the electron trap depth.

Discussion

These calculations show that the site of adsorption on the crystal surface is important in determining silver cluster electronic properties. We have chosen sites thought to be important on cubic surfaces. These sites may be considered in a more general sense as representative of partially charged sites. The cluster energy levels behave as if a partial site charge can exist on the surface. For example, the calculated IP and EA values are largest at the positive kink and become smaller as one moves to the neutral double kink and flat surface or the negative kink. This is a localized effect that is fully consistent with the proposals of Seitz[36] as incorporated in the nucleation and growth model.[1–3] In that model the positive kink was assigned an important role in trapping photoelectrons and in their conversion to silver clusters. This pathway always has a partial charge that could alternately attract silver ions or electrons but as these calculations show the clusters do not monotonically form a deeper trap for electrons but do increase in overall stability. All of the silver clusters Ag_1 to Ag_4 can trap photoelectrons due to their EA values, which exceed the crystal EA. These are not necessarily permanent traps for electrons and require the addition of an interstitial silver ion to stabilize the electron. There are oscillations in the IP and EA of the adsorbed clusters that can be understood on the basis of open and closed shell electron pairs. In this regard Ag_3 is rather unstable. Its IP is relatively small and EA is relatively large. Thus, it is an energetically favored trap for holes or electrons. But Ag and Ag_2 have large IP values, which make them stable against electron release to the conduction band. At the other sites such as -DK, flat, and –K many of the neutral clusters have an ability to trap photoholes, but not photoelectrons. The trends observed in both *ab initio* and CNDO calculations correlate well with one another on the above points.

Strong coupling of electrons to the silver halide crystal lattice has generally been considered unimportant. The hole forms a stable self-trapped state in AgCl and metastable in AgBr, but no corresponding state was known for the electron. Hamilton[2,20,21] presented arguments in favor of the strong coupling proposal based upon an explanation of comparable recombination and electron trapping rates. We find evidence for this type of electron trap deepening in these calculations. Trapping of electrons at a silver cluster on a surface site causes a change in the geometry of the cluster and leads to an increased trap depth of several tenths of an electron volt.

Gold has been considered to increase the developability of silver halide. One study[37] comparing critical sizes for development showed that Au_2 or Ag_4 were required for development. It was thought that the gold clusters had larger EA values than silver clusters as a possible explanation for this behavior. Our calculations support the proposal of larger EA values for the gold clusters than silver clusters.

It is generally agreed that the space charge potential is negative at room temperature for AgCl and AgBr. Interpretations of experiments require models for the surface defects, and so it has been difficult to determine precise values of this potential. The negative kinks are thought to be in excess concentration at these surfaces and thus responsible for the sign of the potential. Our calculations indicate that the energy of converting positive kinks to negative kinks with interstitial formation is less than the energy of the corresponding vacancy formation reaction. This result is consistent with the experimental potential, but entropy effects should be included in a complete analysis.

We have applied the well suited computational methods capable of treating local bonding and long-range lattice polarization and interpreted the results in the framework of accepted mechanisms of latent image formation. Yet we know this is an extremely complicated problem. The surface of the photographic grain where a latent image form is not fully characterized. This fact coupled with possible sources of error in the calculation itself should be remembered. For this reason we present the theoretical results coupled closely to experimental understanding rather than as a stand-alone entity. We expect that, together, experiment and theory of the type presented here can advance our understanding of microscopic mechanisms of the photographic process.

References

1. T. H. James, *The Theory of the Photographic Process*, 4th ed., MacMillan, New York, 1977.
2. J. F. Hamilton, The silver halide photographic process, *Adv. Phys.* **37,** 359 (1988).
3. T. Tani, *Photographic Sensitivity*, Oxford, New York, 1995.
4. A. P. Marchetti and R. S. Eachus, The photochemistry and photophysics of the silver halides, *Adv. Photochem.* **17,** 145 (1992).
5. (a) R. C. Baetzold, Properties of silver clusters on AgBr surface sites, *Photogr. Sci. Eng.* **19,** 11 (1975); (b) R. C. Baetzold, Electronic effects in silver latent image particles, *J. Photogr. Sci.* **28,** 15 (1980).
6. J. F. Hamilton, and R. C. Baetzold, The paradox of Ag_2 centers on AgBr: Reduction sensitization versus photolysis, *Photogr. Sci. Eng.* **25,** 189 (1981).
7. E. Moisar and F. Granzer, Formation, nature, and action of sensitivity centers and latent image specks, *Photogr. Sci. Eng.* **26,** 1 (1981).
8. J. Flad, H. Stoll, A. Niklass, and H. Preuss, Quantum chemical investigations of the latent image formation, *Z. Phys. D* **15,** 79 (1990).
9. F. Dietz, A. Koch, C. Nieke, R. Richter, J. Reinhold, A. Tadjer, and N. Tyutyulkov, Quantum chemical investigations of the mechanisms of the photographic process III, *J. Imaging Sci.* **30,** 146 (1986).
10. K. B. Shelimov, A. A. Safonov, and A. A. Bagaturyants, *Ab initio* calculations of a M center on the AgBr (100) surface, *Chem. Phys. Lett.* **201,** 84 (1993).
11. J. W. Mitchell, The stable latent image, *Photogr. Sci. Eng.* **22,** 1 (1978).
12. M. R. V. Sahyun, Towards a quantum chemical model of the photographic process, *Photog. Sci. Eng.* **22,** 317 (1978).
13. H. E. Spencer, L. E. Brady, and J. F. Hamilton, Study of the mechanism of sulfur sensitization by a development-center technique, *J. Opt. Soc. Am.* **57,** 1020 (1967).
14. H. E. Spencer, Reactions of electrons and holes in latent image formation, *Photogr. Sci. Eng.* **11,** 352 (1967).
15. T. Tani, Photographic effects of electron and positive hole traps, *Photogr. Sci. Eng.* **15,** 28 (1971).

16. T. Tani, Physics of the photographic latent image, *Phys. Today* **36,** 36 (1989).
17. T. Tani and M. Murofushi, Silver microclusters on silver halide grains as latent image and reduction sensitization centers, *J. Imaging Sci. Technol.* **38,** 1 (1994).
18. S. Guo and R. K. Hailstone, Spectroscopic and sensitometric studies of chemically produced silver clusters, *J. Imaging Sci. Technol.* **40,** 210 (1996).
19. R. K. Hailstone, Computer simulation studies of silver cluster formation on AgBr microcrystals, *J. Phys. Chem.* **99,** 4414 (1995).
20. J. F. Hamilton, Toward a quantitative latent-image theory, *Photogr. Sci. Eng.* **26,** 263 (1982).
21. J. F. Hamilton, The case for strong electron-lattice coupling at photographic centers in the silver halides, *J. Imaging Sci.* **34,** 1 (1990).
22. C. R. A. Catlow and W. C. Mackrodt, *Computer Simulation of Solids*, Springer, Berlin, 1982.
23. A. M. Stoneham, *Theory of Defects in Solids*, Clarendon, Oxford, 1975.
24. (a) P. W. M. Jacobs, J. Corish and C. R. A. Catlow, Calculation of the Frenkel defect formation energy in silver chloride, *J. Phys. C.* **13,** 1980 (1977); (b) P. W. M. Jacobs, The calculation of defect energies in silver halides, *J. Imaging Sci. Technol.* **34,** 79 (1990); (c) R. C. Baetzold, C. R. A. Catlow, J. Corish, F. M. Healy, P.W. M. Jacobs, M. Leslie, and Y. T. Tan, The effects of three-body interactions on crystal properties and defect energies in silver halides, *J. Phys. Chem. Sol.* **50,** 791 (1989); (d) C. R. A. Catlow, J. Corish, J. H. Harding, and P. W. M. Jacobs, A calculation of defect Gibbs energies for silver chloride and silver bromide, *Philos. Mag. A* **55,** 481 (1987).
25. N. F. Mott and M. J. Littleton, Conduction in polar crystals. I. Electrolytic conduction in solid salts, *Trans. Faraday Soc.* **34,** 481 (1938).
26. (a) P. W. Tasker, Computer simulation of defects in ionic solids, *Philos. Mag. A* **39,** 119 (1979); (b) J. H. Harding, The surface energies, surface tensions and surface structure of the alkali halide crystals, *Rep. Prog. Phys.* **53,** 1403 (1990).
27. R. C. Baetzold, Computation of the energetics of surface vacancy and interstitial generation in silver halide, *Phys. Rev. B* **52,** 114, 24 (1995).
28. (a) A. D. Becke, Density-functional exchange-energy approximation with correct asymptotic behavior, *Phys. Rev. A* **33,** 3098 (1988); (b) C. Lee, W. Yang, and R. G. Parr, Development of the Colle-Salvetti correlation-energy formula into a functional of the electron density, *Phys. Rev. B* **37,** 785 (1988).
29. Y. Sakai, E. Miyoshi, M. Klobukwski, and S. Huzinaga, Model potentials for molecular calculations II, *J. Comput. Chem.* **8,** 256 (1987).
30. R. C. Baetzold and R. S. Eachus, The possibility of a split-interstitial silver ion in AgCl, *J. Phys. Condens. Mater.* **7,** 3991 (1995).
31. CADPAC: The Cambridge Analytical Derivatives Package Issue 6, Cambridge (1995). A suite of quantum chemistry programs developed by R. D. Amos with contributions from I. L. Alberts, J. S. Andrews, S. M. Colwell, N. C. Handy, D. Jayatilaka, P. M. Knowles, R. Kobayashi, K. E. Laidig, G. Laming, A. M. Lee, P. E. Maslen, C. W. Murray, J. E. Rice, E. D. Semandiras, A. J. Stone, M. D. Sei, and D. J. Tozer.
32. R. C. Baetzold, Calculated properties of Ag clusters on silver halide cubic surface sites, *J. Phys. Chem.* **101,** 8180 (1997).
33. D. M. Duffy, J. P. Hoare and P. W. Tasker, Vacancy formation energies near the surface of an ionic crystal, *J. Phys. C.* **17,** L195 (1984).
34. J. H. Webb, Low-intensity reciprocity-low failure in photographic exposure, *J. Opt. Soc. Am.* **23,** 157 (1933).
35. M. Kawasaki and H. Hada, Lifetime of the photolytic silver atom in silver halide photographic emulsion, *J. Imaging Sci.* **29,** 132 (1985).
36. F. Seitz, Speculations on the properties of the silver halide crystals, *Rev. Mod. Phys.* **23,** 328 (1951).
37. J. F. Hamilton and P. C. Logel, The minimum size of silver and gold nuclei for silver physical development, *Photog. Sci. Eng.* **18,** 507 (1974).